

# Computer Aided Diagnosis system for Parkinson's disease detection based on Histogram Equalization and Support Vector Machine

Safouane Hamdi<sup>1</sup>, Olfa Laouini<sup>2,3</sup>

<sup>1</sup> University of Sfax, National School of Electronics and Telecommunications, Department of Telecommunications, Tunisia.

<sup>2</sup> University of Tunis El Manar, Faculty of Medicine, Department of Biophysics, Tunisia

<sup>3</sup> University of Tunis, Higher National Engineering School, Center of Research in productivity and image processing, Tunisia

[1safouanehamdy@gmail.com](mailto:safouanehamdy@gmail.com) , [23olfa.laouini@gmail.com](mailto:olfa.laouini@gmail.com)

**Abstract**— Parkinson's disease (PD) is a chronic neurodegenerative disorder occurs at the central nervous system. PD involves the malfunction or death of certain vital cells in the brain called neurons. The factor, which affects the quality of life of patients. Still there is no particular test to detect the disorder at an early stage. In fact, physicians rely mainly on functional neuroimaging to identify abnormalities in cerebral activity. Despite its wide qualities, such an imaging modality yields voluminous and ambiguous output. To examine properly these large amounts of data, experts face various constraints, including short available time and insufficient relevant information. Recently, new developments in machine learning and computer vision have led to the occurrence of a new concept known by Computer Aided Diagnosis (CAD). CAD is used to improve the diagnosis of a wide variety of lesions and tumors. It assists doctors make the proper decision. In this paper, a new CAD system based on Histogram Equalization (HE) as a preprocessing technique is performed. The effect of applying HE on the images is studied by determining the difference between the probability distributions of each image before and after normalization and the mean of all normalized images. To extract the most pertinent data, two methods, including Voxels as Features (VAF) and Principal Component Analysis (PCA) are used. The extracted features will be used as input data for a classifier. Finally, to identify the subjects suspected of being affected by PD, a Support Vector Machine (SVM) is trained. The proposed methodologies are tested on a 40 DaTSCAN images database from Parkinson Progression Markers Initiative (PPMI). High accuracy rates with peaks of 91, 37% for VAF and 92, 93% for PCA, are achieved.

**Index Terms**— Computer Aided Diagnosis (CAD), DaTSCAN, Histogram Equalization (HE), Parkinson's disease (PD), Principal Component Analysis (PCA), Support Vector Machine (SVM).

## 1 INTRODUCTION

PARKINSON'S disease (PD) is a long-term degenerative disorder, occurs at the central nervous system. It affects the motor system by mainly causing tremors, slow movements, rigid muscles and postural instability. The motor symptoms of the disorder result from the deterioration of certain cells called neurons. These cells are concentrated in the substantia nigra, a region of the midbrain. The main function of neurons is to produce dopamine. Dopamine is a chemical, which transmits messages between the substantia nigra and other parts of the brain. The factor that keeps smooth and coordinated muscles. When approximately 60% to 80% of the dopamine-producing cells are damaged, the motor symptoms of PD begin to appear [1].

There is as yet no particular test to clearly detect the disorder. In order to visualize the loss of dopamine, functional neuroimaging is found to be very efficient. A common technique, such as Single-Photon Emission Computed Tomography (SPECT) is widely applied in PD diagnosis. SPECT not only provides an anatomical vision of the brain but also shows which areas are more or less active than a regular threshold. SPECT mainly uses a radiotracer called Ioflupane (<sup>123</sup>I) (better known as DaTSCAN). It is injected into the patient's vein and observed with a gamma camera in order to detect abnormal levels of radioactivity in the brain. Usually, in such an imaging modality,

several constraints are to be faced. Limited time of diagnosis, voluminous data and lack of pertinent information are the most frequent obstacles on the way to the proper diagnosis of PD.

Due to the progressive advances in computing and digital imaging, an increasing interest in performing new automated predictive systems has been viewed. These advances have led to the emergence of Computer Aided Diagnosis (CAD). CAD is an interdisciplinary technology, which combines various elements of artificial intelligence [2, 3, 4], computer vision [5, 6] and radiological image processing [4]. CAD can be applied to all imaging modalities as well as for all body parts [7]. CAD technology has become one of the major research subjects in medical imaging and diagnostic radiology. In fact, a large number of CAD models for several neurodegenerative disorders, such as Alzheimer's disease [8, 9, 10, 11, 12, 13] and PD [14, 15] have been lately developed.

In this work, a new CAD system, as described in Fig. 1 is carried out. We will make use of 40 DaTSCAN SPECT images from Parkinson Progression Markers Initiative (PPMI), including 20 Normal Control subjects (NCs) and 20 Parkinson's disease subjects (PDs). The images are spatially normalized using SPM8. The intensity normalization is done using Histogram Equalization (HE). The effect of HE on the images is shown by

determining the distance between each image before and after normalization and the mean of all normalized images. The measurements are carried out using two statistical measures, Kullback–Leibler divergence (KLD) and Jeffery Divergence (JD). Then, to extract the most relevant data, we will make use of two features extraction techniques, Voxels as Features (VAF) and Principal Component Analysis (PCA). VAF involves the use of all voxels in each image as a feature vector. PCA is used to reduce the dimensions of the feature space. The classification is made using Support Vector Machine (SVM) for both methods of feature extraction.

This paper is organised as follows: in section 2, an overview of HE, PCA and SVM is described. Section 3 presents the material and methods adopted in the present work. Section 4 discusses the results. Finally, the conclusion is drawn in Section 5.

## 2 BACKGROUND

### 2.1 Histogram Equalization (HE)

Histogram Equalization (HE) is a technique for adjusting an image intensity and enhancing its contrast. HE is not about changing the values contained in the matrix  $X(m, n)$ , which represents the image. Instead, it modifies the color mapping associated with the values of the matrix  $X(m, n)$ . So that we tend to use every color in the full dynamic range [black to white] in an equal way.

Consider a discrete grayscale image  $\{x\}$ . Let  $n_i$  be the number of occurrences of gray level  $i$ . The probability of an occurrence of a level  $i$  pixel in the image is:

$$P_x(i) = P(x = i) = \frac{n_i}{n}, \quad 0 \leq i < L \quad (1)$$

$L$  is the total number of gray levels in the image.  $n$  is the total number of pixels in the image.  $P_x(i)$  denotes the image histogram for the pixel value  $i$ , normalized to [0,1].

Consider the cumulative distribution function (which is also the accumulated normalized histogram of the image) corresponding to  $P_x$  as:

$$cdf_x(i) = \sum_{j=0}^i P_x(j) \quad (2)$$

Trying to create a transformation of the form  $y = T(x)$  to produce a new image  $\{y\}$  with a flat histogram. This image has a linearized cumulative distribution function  $cdf$  across the value range:

$$cdf_y(i) = ik \quad (3)$$

Where  $k$  is a constant. The properties of  $cdf$  allow us to perform a transform, which is defined as:

$$cdf_y(y') = cdf_y(T(k)) = cdf_x(k) \quad (4)$$

Where  $k$  is in the range  $[0, L)$ . Notice that  $T$  maps the levels into the range  $[0, 1]$ , since a normalized histogram of  $\{x\}$  has been used. In order to map the values back into their original range, the following simple transformation needs to be applied on the result:

$$y' = y \cdot (\max\{x\} - \min\{x\}) + \min\{x\} \quad (5)$$

### 2.2 Principal Component Analysis (PCA)

Principal Component Analysis (PCA) is a procedure for identifying a smaller number of uncorrelated variables, called "principal components" from a large set of data. It is used to explain the maximum amount of variance with the fewest number of principal components.

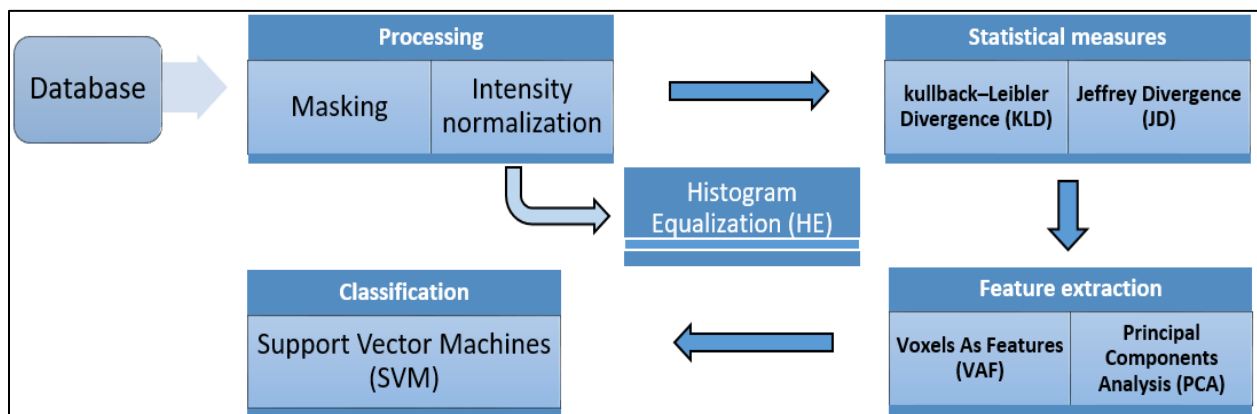


Fig. 1. Flow Chart of the proposed methodologies.

Mathematically, PCA is defined as an orthogonal linear transformation that transforms the data into a new coordinate system. So that, the greatest variance by projection of the data comes to lie on the first coordinate (first principal component). The second greatest variance comes to lie on the second coordinate (second principal component), and so on.

Consider two matrices:  $e_i = \begin{pmatrix} e_{i1} \\ e_{i2} \\ \vdots \\ e_{ip} \end{pmatrix}$ ,  $X = \begin{pmatrix} X_1 \\ X_2 \\ \vdots \\ X_p \end{pmatrix}$

Where  $e_i$  denotes a coefficients matrix,  $X$  denotes a data matrix.

Consider the population variance matrix of  $X$  :

$$var(X) = \sum = \begin{pmatrix} \sigma_{11} & \sigma_{12} & \cdots & \sigma_{1p} \\ \sigma_{21} & \sigma_{22} & \cdots & \sigma_{2p} \\ \vdots & \vdots & \ddots & \vdots \\ \sigma_{p1} & \sigma_{p2} & \cdots & \sigma_{pp} \end{pmatrix} \quad (6)$$

Consider the linear combination:

$$Y_{i=\{1...p\}} = e_{i1}X_1 + e_{i2}X_2 + \dots + e_{ip}X_p \quad (7)$$

Consider the population variance of  $Y_i$  as:

$$var(Y_i) = \sum_{k=1}^p \sum_{l=1}^p e_{ik}e_{il}\sigma_{kl} = e_i'\Sigma e_i \quad (8)$$

**The first principal component ( $Y_1$ )** is the linear combination of x-variables, which has the maximum variance (among all linear combinations). Specifically we will select  $e_{11}, e_{12}, \dots, e_{1p}$  that maximize:

$$var(Y_1) = \sum_{k=1}^p \sum_{l=1}^p e_{1k}e_{1l}\sigma_{kl} = e_1'\Sigma e_1 \quad (9)$$

**The second principal component ( $Y_2$ )** is the linear combination of x-variables, which has the maximum variance (among all linear combinations). Specifically we will select  $e_{21}, e_{22}, \dots, e_{2p}$  that maximize:

$$var(Y_2) = \sum_{k=1}^p \sum_{l=1}^p e_{2k}e_{2l}\sigma_{kl} = e_2'\Sigma e_2 \quad (10)$$

### 2.3 Support Vector Machine (SVM)

Support Vector Machine (SVM) was introduced in the late 70s [16]. It is a set of related supervised learning methods widely used in pattern recognition [17], voice activity detection [18] and classification [13]. SVM with linear discriminant functions defines decision hypersurfaces or hyperplanes in a multidimensional feature space, that is:

$$g(x) = W^T X + \omega_0 = 0 \quad (11)$$

Where  $W$  is known as the weight vector and  $\omega_0$  as the threshold. The weight vector  $W$  is orthogonal to the decision hyperplane. The optimization task consists of finding the unknown parameters  $\omega_{i=\{1,...,n\}}$  that define the decision hyperplane.  $X_{i=\{1,...,n\}}$  are the feature vectors of the training set  $X$ .

## 3 MATERIAL AND METHODS

### 3.1 Material

To evaluate the performance of the proposed methodologies, we made use of a 40 SPECT images database, as illustrated in Fig. 2, which were obtained from Parkinson Progression Markers Initiative (PPMI). The images included in our database were imaged 4 + 0.5 h after the injection of between 111 and 185 MBq of DaTSCAN. Subjects were also preprocessed with saturated iodine solution (10 drops in water) or perchlorate (1000 mg) prior to the injection. All subjects had a supplied 57 Commitment ordering line marker affixed along the canthomeatal line, which will facilitate subsequent image processing and allows the core lab to accurately distinguish left and right in the face of multiple image file transfers.

After processing, our database contains 40 images, 20 from Normal Control subjects (NCs) and 20 from PD subjects (PDs). The images are 69\*95\*79 of size.

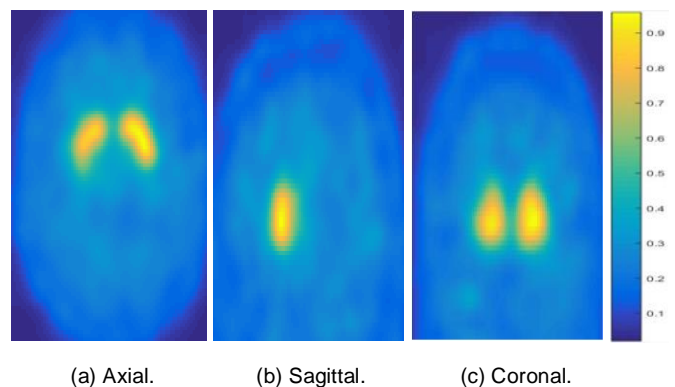


Fig.2. Template image generated by averaging the NCs.

### 3.2 Methods

#### 3.2.1 Spatial normalization

Spatial normalization is a kind of image registration. The location of the brain scan of a given subject can be correlated to the same location as the brain scan of another subject. All the images of the available database were already registered and spatially normalized using SPM8 software.

#### 3.2.2 Masking

In order to differentiate the Region of Interest (RoI) (related to dopamine transporters in the striatum) from Non-Specific Regions (NSR), several binary masks were created. These masks, as shown in Fig. 3 (a), Fig. 3 (b) and Fig. 3 (c) select all voxels that are higher than a specific intensity threshold  $I_{th}$ . So that, only selected voxels are considered in further processing. The threshold is established as the mean value of the intensity in the entire image and computed as follows:

$$I_{th} = 0.45 \times I_{max} \quad (12)$$

$$I_{max} = \max(I_{mean}(:)) \quad (13)$$

Where  $I_{mean}$  is the average image.  $I_{max}$  is the maximum intensity of  $I_{mean}$ . The resulting masks illustrate the selection of the discriminative region of PD, as demonstrated in Fig. 3 (d), Fig. 3 (e) and Fig. 3 (f).

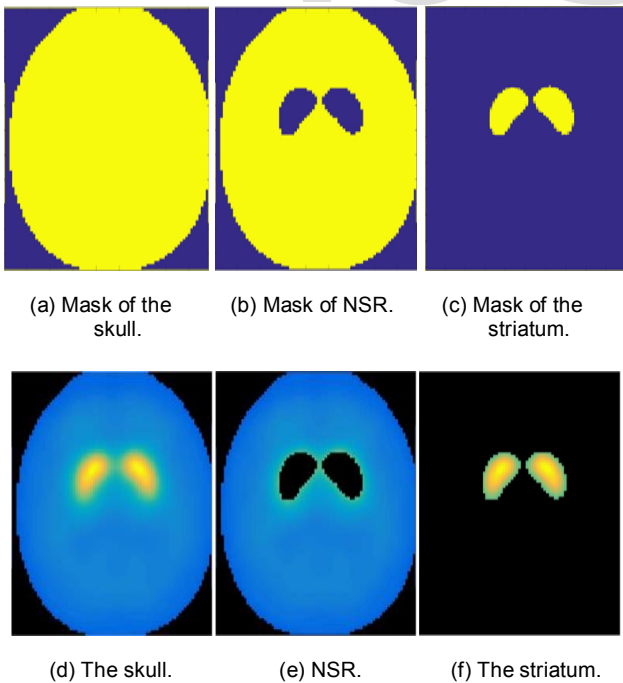


Fig. 3. Selection of RoI using binary masks.

#### 3.2.3 Intensity normalization

In order to determine the activity in the RoI, a certain kind of intensity normalization is required. For this reason, we made use of Histogram Equalization (HE).

First, HE was applied on the entire image, including RoI and NSR. Then, it was applied only in NSR keeping the original striatum signal.

#### 3.2.4 Statistical measures

We can never be completely certain that a given relationship really exists between two distributions. There are various sources of error to be controlled, such as sampling error, researcher bias, problems with reliability and validity. Statistical measures are used to determine what is the probability that the relationship we think we have found is due only to random chance. We made use of two statistical measures, Kullback-Leibler Divergence (KLD) and Jeffrey Divergence (JD). These measures are carried out to study the difference between the probability distributions of all images before and after normalization and the mean of all normalized images.

##### 3.2.4.1 Kullback-Leibler Divergence (KLD)

Also known as (Relative Entropy). It is a non-symmetric measure of the difference between two probability distributions  $\Omega_1$  and  $\Omega_2$ . KLD is defined as:

$$D_{KLD}(\Omega_1, \Omega_2) = \sum_i \Omega_1(i) \log \frac{\Omega_1(i)}{\Omega_2(i)} \quad (14)$$

Where  $\Omega_1$  and  $\Omega_2$  are two discrete random variables. In our case,  $\Omega_1$  denotes the mean of all subjects normalized.  $\Omega_2$  denotes a defined subject before and after normalization.

##### 3.2.4.2 Jeffrey Divergence (JD)

A major weakness of KLD is its non-symmetry. JD is a simple way of making KLD symmetric. It is given by:

$$D_{JD}(\Omega_1, \Omega_2) = D_{KLD}(\Omega_1, \Omega_2) + D_{KLD}(\Omega_2, \Omega_1) \quad (15)$$

$$D_{JD}(\Omega_1, \Omega_2) = \sum_i \Omega_1(i) \log \frac{\Omega_1(i)}{\Omega_2(i)} + \sum_i \Omega_2(i) \log \frac{\Omega_2(i)}{\Omega_1(i)} \quad (16)$$

Where  $\Omega_1$  and  $\Omega_2$  are two discrete random variables.  $i$  denotes an element of the probability distribution  $\Omega$ . This distance solves the non-symmetry issue in a very simple and intuitive way.



### 3.2.5 Feature extraction

Feature extraction is aimed to obtain the most relevant information from an original voluminous space and to present this information in a lower dimensional space. Thus, it transforms the original data space of high dimension into another space with a reduced dimension to obtain new better features. In this work, two feature extraction techniques was used:

**Voxels as Features (VAF):** is considered as a baseline in many works as many studies suggest that this method is, at least, comparable with the visual exam performed by experts [19]. This approach uses all voxels in each image as input features to train a classifier.

**Principal Component Analysis (PCA):** is a procedure for identifying a smaller number of uncorrelated variables, called principal components from a large data set. The objective of PCA is to explain the maximum amount of variance with the fewest number of principal components. PCA has achieved good results when applied to other conditions, such as breast cancer [20, 21, 22] and Alzheimer’s Disease [23, 24].

### 3.2.6 Classification

The vectors extracted using VAF and PCA are both used by a linear classifier. The classification is performed using Support Vector Machine (SVM). SVM is a powerful algorithmic tool that is able to separate a set of binary-labelled training data with a hyperplane, which is maximally distant from the two classes.

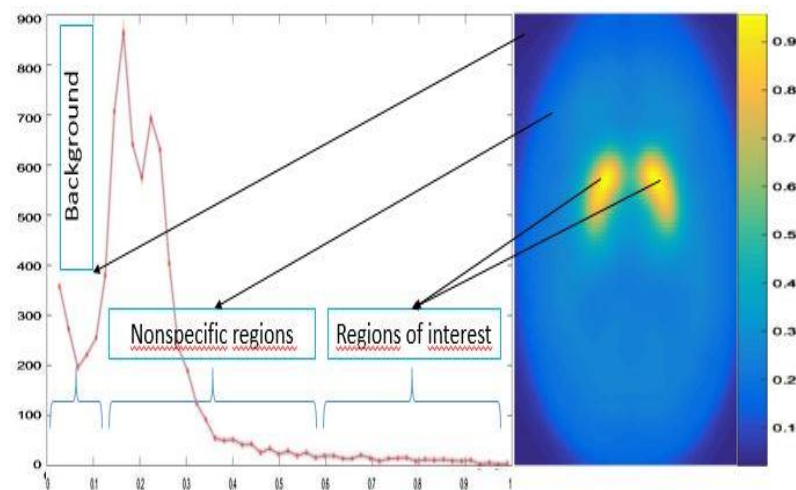
## 4 RESULTS AND DISCUSSION

### 4.1 Qualitative analysis

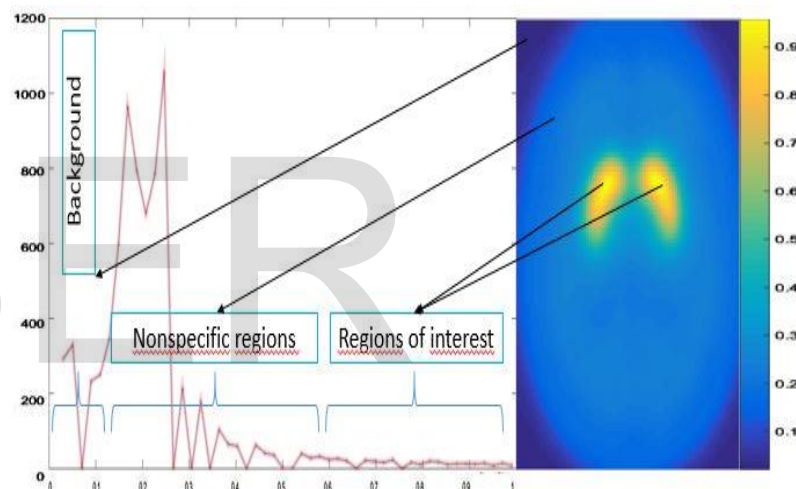
After creating the three masks described in Fig. 3, the significant areas of the images were specified and distinguished. The distinction of regions is based on their voxels intensity values.

Fig. 4 shows the effect of applying HE on a DaTSCAN image belongs to Normal Control subjects (NCs). It describes the image histogram for each approach of intensity normalization. Furthermore, Fig. 4 identifies the specific and nonspecific areas, their intensity values and their locations. The right end region characterized by high intensity values correspond to the RoI. The peaks of intensity shown in the left half of the histograms are due to the fact that most of the NSR voxels have very similar intensity values. The left end region characterized by the lowest intensity values belongs to the image background (non-relevant data).

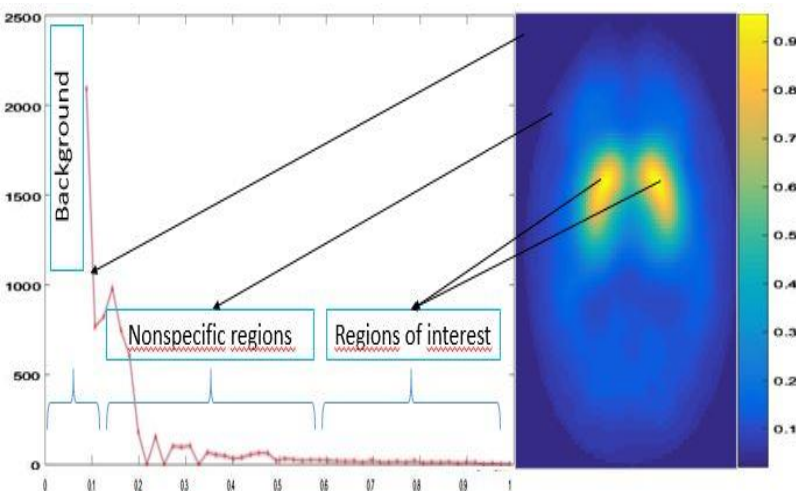
Fig. 4 (a) shows the original image and its associated histogram, which indicates the intensity distribution for each region. In Fig. 4 (b), HE was applied over the entire image. Applying HE involves the reduction of noise and artifacts, which affects the source image. The noise is assumed to be from the Gaussian noise. Thus, this approach entails an enhancement of signal-to-



(a) Original image.



(b) Image normalized in all regions.



(c) Image normalized in NSR.

Fig. 4. The effect of applying HE on a DaTSCAN image.

noise ratio (SNR). Although SNR increased, the striatum still not obviously identified. The factor, which makes the diagnosis of PD ineffective. This is explained by the fact that HE also affects the RoI that refers to the striatum. Therefore, the differentiation between the two classes, NCs and PDs becomes harder. For this reason, we tried to apply HE only in NSR. In Fig. 4 (c), only NSR were normalized keeping the original striatum signal. In fact, the striatum, which is the key area used to make a visual diagnosis of PD is clearly highlighted.

## 4.2 Quantitative analysis

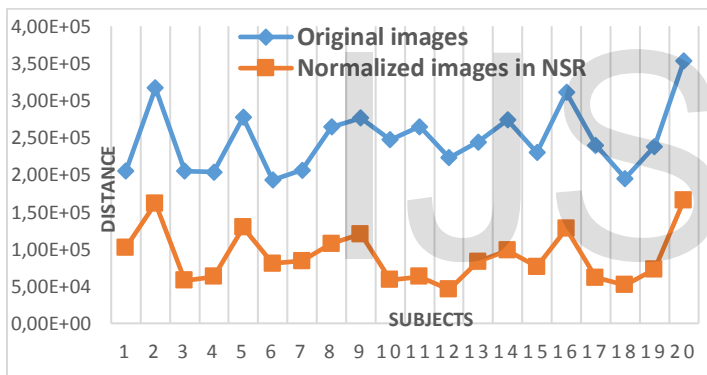
### 4.2.1 Statistical measures

Fig. 5 shows the inter-subject distance between 40 subjects (20 NCs and 20 PDs) before and after normalization and the mean of all normalized images. The distances were determined using two statistical measures (KLD and JD). After applying HE, the inter-subject distance decreased. This is due to the normalization, which enhances contrast and eliminates noise.

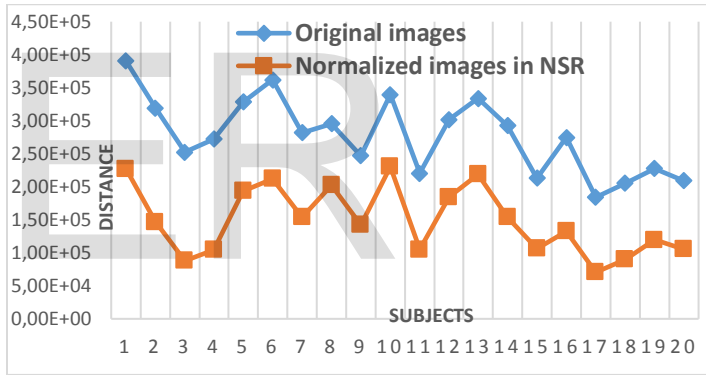
### 4.2.2 Classification

Firstly, the classification was performed using VAF. In fact, all voxels of the image were used as a feature vector. Then, this vector had to be the input of an SVM classifier. Table 1 presents the accuracy rates achieved for the different approaches of intensity normalization while using VAF for feature extraction. As indicated in Table 1, applying HE on NSR improves the classification rates with peaks of 91.37%, 90.34% and 91.63% for accuracy, sensitivity and specificity, respectively.

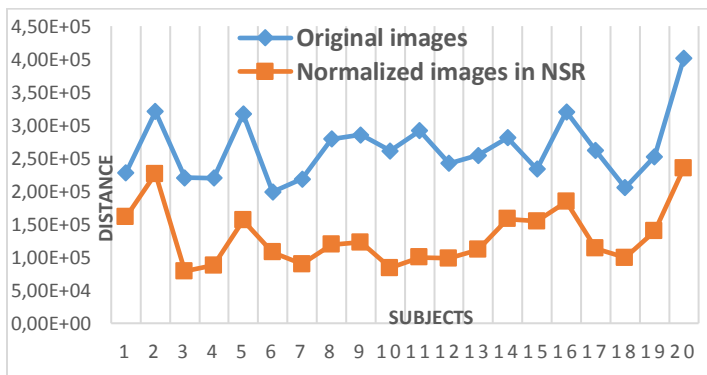
Secondly, to extract the most relevant data, we made use of PCA. As shown in Table 2, the proposed methodologies provide high accuracy rates for PD diagnosis. A peak of over 92.93% is achieved. Normalizing the images in NSR represents a significant improvement in the accuracy rates compared to those obtained by original images and normalized images in all regions. The improvement in accuracy is due to the ability of PCA to extract the patterns that explain the greater variance in the data. In addition, the dimensional reduction of PCA is very effective in classification.



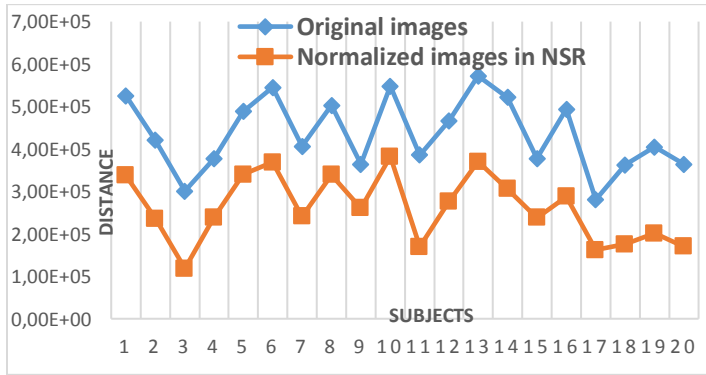
(a) KLD distances of NCs.



(b) KLD distances of PDs.



(c) JD distances of PDs.



(d) JD distances of NCs.

Fig. 5. The variation of distance between each subject before and after normalization and the mean of all normalized images.

The proposed methodologies performed several previous similar efforts in terms of accuracy. Table 3 evaluates the accuracy rate achieved in this paper compared to those achieved by several similar works. The present work shares with Martínez-Murcia et al [25] several techniques, including database, statistical measures and classification. In addition, several common features, such as database, feature extraction and classification make the link with the work of Brahim et al [26].

TABLE 1  
ACCURACY RATES ACHIEVED USING VAF

	Accuracy	Sensitivity	Specificity
Original image	86,85 %	85,79 %	87,77 %
Normalization in all regions	87,98 %	87,65 %	88,89 %
Normalization in NSR	91,37 %	90,34 %	91,63 %

TABLE 2  
ACCURACY RATES ACHIEVED USING PCA

	Accuracy	Sensitivity	Specificity
Original image	89,47 %	89,14 %	88,39 %
Normalization in all regions	89,98 %	90,08 %	89,83 %
Normalization in NSR	92,93 %	91,25 %	93,13 %

## 5 CONCLUSION

In the preprocessing step, the images have been spatially normalized using SPM8. Then, in order to distinguish the different regions of images, three binary masks have been created and applied to the spatially normalized dataset. Finally, two approaches of intensity normalization using Histogram Equalization (HE) have been applied. The first approach aims to normalize images in all regions, the second approach involves normalizing images just in Non-Specific Regions (NSR). To highlight the effect of HE on both approaches of normalization, we have performed two statistical measures Kullback-Leibler Divergence (KLD) and Jeffrey Divergence (JD). KLD and JD have been executed to study the difference between the probability distributions of each image before and after normalization and the mean of all normalized images. Thereafter, two feature extraction techniques, including Voxels as Features (VAF) and Principal Component Analysis (PCA) have been used. VAF and

PCA are aimed to extract the most relevant features and present this data in a lower dimensional space, which will work as a feature vector. Finally, an SVM classifier has been trained to detect PD patterns and to evaluate the performance of our proposed methodologies.

TABLE 3  
COMPARISON BETWEEN THE ACCURACY RATES ACHIEVED IN THIS WORK AND THOSE PERFORMED BY SEVERAL PREVIOUS WORKS THAT SHARE MULTIPLE COMMON MATERIAL OR METHODS

Paper	Accuracy rate	Common material / methods
The present work	92.93%	
Martínez-Murcia et al [25]	91.3%	Database Statistical measures Classifier
Brahim et al [26]	92.91%	Database Feature extraction Classifier

## REFERENCES

- [1] J.S. Bridle, "Probabilistic M. M. Goldenberg, "Medical management of Parkinson's disease," Pharmacy and Therapeutics, vol. 33, no. 10, pp. 590-594, October 2008.
- [2] J. Shiraishi, K. Li, D. Appelbaum, and K. Doi, "Computer-aided diagnosis and artificial intelligence in clinical imaging," Semin Nucl Med, vol. 41, no. 6, pp. 449-62, November 2011.
- [3] M. Avneet Pannu, "Artificial Intelligence and its Application in Different Areas," International Journal of Engineering and Innovative Technology (IJEIT), vol. 4, no. 10, April 2015.
- [4] J. Stoitsisa and I. Valavanisa, "Computer Aided Diagnosis Based On Medical Image Processing and Artificial Intelligence Methods," Nuclear Instruments and Methods in Physics Research Section A: Accelerators, Spectrometers, Detectors and Associated Equipment, vol. 569, pp. 591-595, December 2006.
- [5] C. H. Chen, Ed., Computer Vision in Medical Imaging. World Scientific Publishing Co. Pte. Ltd., January 2013, vol. 2.
- [6] R. Beichal and M. Sonka, Eds., Computer Vision Approaches to Medical Image Analysis, 1st ed. Springer-Verlag Berlin Heidelberg, May 2012.
- [7] K. Doi, "Current status and future potential of computer-aided diagnosis in medical imaging," The British Journal of Radiology, vol. 78, no. 1, pp. 3-19, 2005.
- [8] J. Stoeckel, N. Ayache, G. Malandain, P. Koulbaly, K. Ebmeier, and J. Darcourt, "Automatic classification of SPECT images of Alzheimer's disease patients and control subjects," Medical Image Computing and Computer-Assisted Intervention - MICCAI, Lecture Notes in Computer Science, vol. 3217, pp. 654-662, 2004.
- [9] I. A. Illan, J. M. Goriz, J. Ramirez, D. Salas-Gonzalez, M. M. Lopez, F. Segovia, R. Chaves, M. Gomez-Rio, and C. G. Puntonet, "18F-FDG PET

- imaging analysis for computer aided Alzheimer's diagnosis," *Information Sciences: an International journal*, vol. 181, no. 4, pp. 903-916, February 2011.
- [10] G. Fung and J. Stoeckel, "SVM feature selection for classification of SPECT images of Alzheimer's disease using spatial information," *Knowledge and Information Systems*, vol. 11, no. 2, pp. 243-258, February 2007.
- [11] E. Corchado, M. Grana, and M. Woniak, "New trends and application-son hybrid artificial intelligence systems," *Neurocomputing*, vol. 75, no. 1, pp. 61-63, January 2012.
- [12] D. Chyzyk, M. Grana, A. Savio, and J. Maiora, "Hybrid dendritic computing with kernel-LICA applied to Alzheimers disease detection in MRI," *Neurocomputing*, vol. 75, no. 1, pp. 72-77, January 2012.
- [13] F. Martinez-Murcia, J. Gorriz, J. Ramirez, C. Puntonet, and D. Salas-Gonzalez, "Computer Aided Diagnosis tool for Alzheimer's Disease based on Mann-Whitney-Wilcoxon U-Test," *Expert Systems with Applications: An International Journal*, vol. 39, no. 10, pp. 9676-9685, August 2012.
- [14] P. Spetsieris, V. Dhawan, Y. Ma, J. Moeller, M. Mentis, and D. Eidelberg, "Computer Aided Diagnosis of functional brain disorders using PET on a PC based platform," *Engineering in Medicine and Biology: 24th Annual Conference and the Annual Fall Meeting of the Biomedical Engineering Society EMBS/BMES Conference*, Proceedings of the Second Joint, vol. 2, pp. 1107-1108, 2002.
- [15] D. Towey, P. Bain, and K. Nijran, "Automatic classification of 123I-FP-CIT (DaTSCAN) SPECT images," *Nuclear Medicine Communications*, vol. 32, no. 8, pp. 699-707.
- [16] V. Vapnik, "Estimation of Dependences Based on Empirical Data," Springer-Verlag, 1982.
- [17] S. Powell, "Registration and machine learning-based automated segmentation of subcortical and cerebellar brain structures," *NeuroImage*, pp. 238-247, 2008.
- [18] J. Ramirez, "SVM-based speech end point detection using contextual speech features," *Electronics Letters*, pp. 877-879, 2006.
- [19] S. Jonathan, A. Nicholas, and M. Gregoire, "Automatic Classification of SPECT Images of Alzheimer's Disease Patients and Control Subjects," vol. 3217, pp. 654-662, 2004.
- [20] Y.-D. Zhang, S.-H. Wang, G. Liu, and J. Yang, "Computer-aided diagnosis of abnormal breasts in mammogram images by weighted type fractional Fourier transform," *Advances in Mechanical Engineering*, vol. 8, no. 2, pp. 1-11, 2016.
- [21] M. Sarfraz, F. Abu-Amara, and I. Abdel-Qader, "A computer aided detection framework for mammographic images using fisher linear discriminant and nearest neighbor classifier," *Journal of Biomedical Science and Engineering*, vol. 5, pp. 323-329, 2012.
- [22] H. YL, C. DR, J. YR, K. SJ, W. HK, and M. WK, "Computer-aided diagnosis using morphological features for classifying breast lesions on ultrasound," *Ultrasound Obstet Gynecol*, vol. 32, no. 4, pp. 565-72, September 2008.
- [23] S.-T. Yang, J.-D. Lee, C.-H. Huang, and J.-J. Wang, "Computer-Aided Diagnosis of Alzheimers Disease Using Multiple Features with Artificial Neural Network," *PRICAI'10 Proceedings of the 11th Pacific Rim international conference on Trends in artificial intelligence*, pp. 699-705, August 2010.
- [24] M. López, J. Ramírez, J. Górriz, and I. Álvarez, "Computer Aided Diagnosis of Alzheimers Disease Using Principal Component Analysis and Bayesian Classifiers," *The Sixth International Symposium on Neural Networks (ISNN 2009)*, vol. 56, pp. 213-221, 2009.
- [25] F. J. Martínez-Murcia, J. M. Górriz, J. Ramírez, I. A. Illán, and A. Ortiz, "Automatic detection of Parkinsonism using significance measures and component analysis in DaTSCAN imaging," *Neurocomputing*, vol. 126, pp. 58-70, February 2014.
- [26] A. Brahim, J. Ramirez, J. M. Gorriz, L. Khedher, and D. Salas-Gonzalez, "Comparison between Different Intensity Normalization Methods in 123I-Ioflupane Imaging for the Automatic Detection of Parkinsonism," *PLOS ONE*, June 2015.